

What’s the point: Semantic segmentation with point supervision

Amy Bearman
Stanford University
abearman@cs.stanford.edu

Olga Russakovsky
Carnegie Mellon University
olgarus@cmu.edu

Vittorio Ferrari
University of Edinburgh
vittorio.ferrari@ed.ac.uk

Li Fei-Fei
Stanford University
feifeili@cs.stanford.edu

Abstract

The semantic image segmentation task presents a trade-off between test accuracy and the cost of obtaining training annotations. Detailed per-pixel annotations enable training accurate models but are very expensive to obtain; image-level class labels are an order of magnitude cheaper but result in less accurate models. We take a natural step from image-level annotation towards stronger supervision: we ask annotators to point to an object if one exists. We demonstrate that this adds negligible additional annotation cost. We incorporate this point supervision along with a novel objectness potential in the training loss function of a state-of-the-art CNN model. The combined effects of these two extensions is a 12.9% increase in mean intersection over union on the PASCAL VOC 2012 segmentation task compared to a CNN model trained with only image-level labels.

1. Introduction

At the forefront of visual recognition is the question of how to most effectively teach computers about new visual concepts. Algorithms trained from large-scale carefully annotated data enjoy better performance than their weakly supervised counterparts (e.g., [11] versus [39], [6] versus [26], [22] versus [27]); however, obtaining strongly supervised data is very expensive [31, 22].

It is particularly difficult to collect training data for semantic segmentation, i.e. the task of assigning a class label to every pixel in the image. Strongly supervised methods require a training set of images with per-pixel annotations [34, 23, 16, 9, 6, 12] (Fig. 1b). Providing an accurate outline of a single object takes between 54 seconds [18] and 79 seconds [22]. A typical indoor scene contains 23 objects [13], raising the annotation cost to tens of minutes per image. Methods have been developed to reduce the annota-

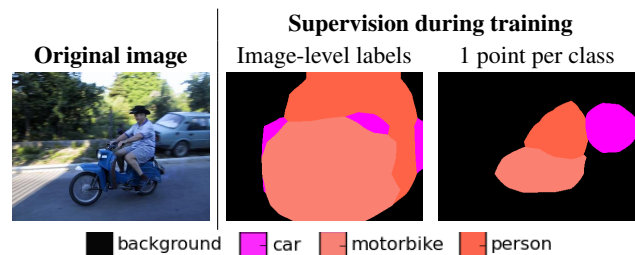


Figure 1: Annotation times for image-level labels vs. single point supervision are both small, but models trained on a single point with the added objectness prior perform significantly better. The second two columns show segmentation results at test time.

tion cost through effective interfaces [30, 21, 22, 41, 3], e.g., through requesting human feedback only as necessary [18]. Nevertheless, accurate per-pixel image annotations remain costly and scarce.

To alleviate the need for large-scale detailed annotations, weakly supervised semantic segmentation techniques have been developed. The most common setting is where only image-level labels for the presence or absence of classes are provided during training [37, 38, 35, 26, 28, 40, 29] (Fig. 2), but other forms of weak supervision have been explored as well, such as bounding box annotations [26], eye tracks [25], free-form squiggles [41] or noisy web tags [1]. These methods require significantly less annotation effort during training, but are not able to segment new images nearly as accurately as fully supervised techniques.

In this work, we take a natural step towards stronger supervision for semantic segmentation at negligible additional cost, compared to image-level labels. The most natural way for humans to refer to an object is by pointing: “That cat over there (*point*)” or “What is that over there? (*point*).” Psychology research has indicated that humans point to objects in a consistent and predictable way [10, 6]. As well,

the fields of robotics [16, 33] and human-computer interaction [23] have long used pointing as the effective means of communication. However, point annotation is largely unexplored in semantic segmentation.

Our **primary contribution** is a novel supervision regime for semantic segmentation based on humans pointing to objects. We extend a state-of-the-art convolutional neural network (CNN) framework for semantic segmentation [22, 28] to incorporate point supervision in its training loss function. With just one annotated point per object class, we considerably improve semantic segmentation accuracy. We ran an extensive human study to collect these points on the PASCAL VOC 2012 dataset, evaluated the annotation times, and will make them available to the community.

One lingering concern with supervision at the point level is that it is difficult to infer the full extent of the object. Our **secondary contribution** is thus incorporating a generic objectness prior [2] directly in the loss, in order to guide the training of a CNN. This prior helps separate objects (e.g., car, sheep, bird) from background (e.g., grass, sky, water), by providing a probability that a pixel belongs to an object (Fig. 2). Such priors have been used in segmentation literature for selecting image regions to segment [15], as unary potentials in a conditional random field model [37], or during inference [29]. However, to the best of our knowledge, we are the first to employ this directly in the loss, in order to guide the training of a CNN.

The combined effects of our contributions is a substantial increase of 12.9% mean intersection over union on the PASCAL VOC 2012 dataset [8] compared to training with image-level labels.

2. Related Work

Types of supervision for semantic segmentation. To reduce the up-front annotation cost for semantic segmentation, recent works have focused on training models in a weakly- or semi-supervised setting. Many forms of supervision have been explored, such as eye tracks [25], free-form squiggles [41], noisy web tags [1], or heterogeneous annotations (a large number of image-level labels and a small number of full segmentation masks) [17]. However, the most common settings are image-level labels [29, 26, 28] and bounding boxes [7, 26]. [4, 20, 13] use co-segmentation methods trained from image-level labels to automatically infer the segmentations. [29, 28, 27] train CNNs supervised only with image-level labels by extending the Multiple-Instance Learning (MIL) framework for semantic segmentation. [26, 7] use an EM procedure, which alternates between estimating pixel labels from bounding box annotations and optimizing the parameters of a CNN.

There is a trade-off between cost and accuracy: models trained with higher levels of supervision perform far better than weakly-supervised models, but require large strongly-

supervised datasets, which are costly and scarce. We propose an intermediate form of supervision, using points, which costs negligible additional annotation time to image-level labels, yet achieves better results. [3] also uses point supervision during training, but it trains a patch-level CNN classifier to serve as a unary potential in a CRF, whereas we use point supervision directly during CNN training.

CNNs for segmentation. Recent successes in semantic segmentation have been mostly driven by methods that train CNNs originally built for image classification to assign semantic labels to each pixel in an image [22, 5, 15, 9]. One extension of the fully convolutional network (FCN) architecture developed by [22] is to train a multi-layer deconvolution network end-to-end. [24]. More inventive forms of post-processing have also been developed, such as combining the responses at the final layer of the network with a fully-connected CRF [5]. We develop our approach on top of the basic framework common to many of these methods.

Interactive segmentation. Some semantic segmentation methods are interactive, in that they collect additional annotations at test-time to refine the segmentation. These annotations can be collected as points [39] or free-form squiggles [30]. These methods require additional user input at test-time; in contrast, we collect user points once only, and we use them only during training.

3. Semantic segmentation method

We describe here our approach to using point-level supervision (Fig. 2) for training semantic segmentation models. In Section 4 we will demonstrate that this level of supervision is cheap and efficient to obtain. In our setting (in contrast to [39]), supervised points are provided only on training images. The learned model is then used to segment test images with no additional human input.

Current state-of-the-art semantic segmentation methods [22, 5, 29, 28, 26], both supervised and unsupervised, employ a unified CNN framework. These networks take as input an image of size $W \times H$ and output a $W \times H \times N$ score map, where N is the set of classes the CNN was trained to recognize (Fig. 2). At test time, the score map is converted to per-pixel predictions of size $W \times H$ by either simply taking the maximally scoring class at each pixel [28, 22] or employing more complicated post-processing [29, 5, 26].

Training these models with different levels of supervision requires defining appropriate loss functions in each scenario. We begin by presenting two of the most commonly used in the literature. We then extend them to our setting of point supervision, and to incorporate an objectness prior.

Full supervision. When the class label is available for every pixel during training (Fig. 2), the CNN is commonly

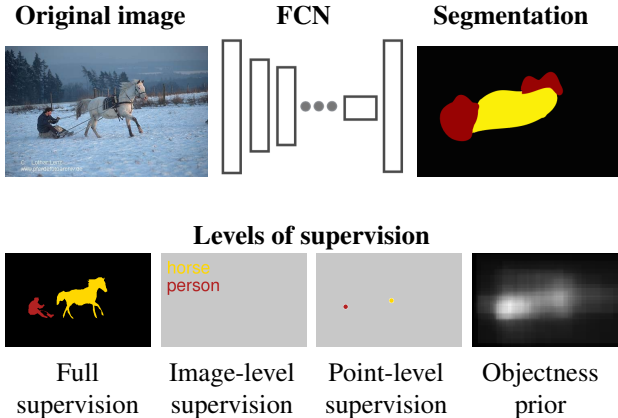


Figure 2: (a) Overview of our semantic segmentation training framework. (b) Different levels of training supervision for semantic segmentation models. For full supervision, the class label of every pixel is provided. For image-level supervision, the class labels are known but their locations are not. We introduce point-level supervision, where each class label is only associated with one or a few pixel(s), corresponding to humans pointing to objects of that class. We include an objectness prior in our training loss function alongside point-level supervision to accurately infer the object extent.

trained by optimizing the sum of per-pixel cross-entropy terms [5, 22]. Let \mathcal{I} be the set of pixels in the image. Let s_{ic} be the CNN score for pixel i and class c . Let $S_{ic} = \exp(s_{ic}) / \sum_{k=1}^N \exp(s_{ik})$ be the softmax probability of class c at pixel i . Given a ground truth map G indicating that pixel i belongs to class G_i , the loss on a single training image is:

$$\mathcal{L}_{pix}(S, G) = - \sum_{i \in \mathcal{I}} \log(S_{iG_i}) \quad (1)$$

The loss is simply zero for pixels where the ground truth label is not defined (for example, in the case of pixels defined as “difficult” on the boundary of objects in PASCAL VOC [8]).

Image-level supervision. In this case, the only information available during training are the sets $L \subseteq \{1, \dots, N\}$ of classes present in the image and $L' \subseteq \{1, \dots, N\}$ of classes not present in the image (Fig. 2). The CNN model can be trained with a different cross-entropy loss:

$$\mathcal{L}_{img}(S, L, L') = - \frac{1}{|L|} \sum_{c \in L} \log(S_{t_c c}) - \frac{1}{|L'|} \sum_{c \in L'} \log(1 - S_{t_c c})$$

with $t_c = \arg \max_{i \in \mathcal{I}} S_{ic}$ (2)

The first part of Eqn. (2), corresponding to $c \in L$, is used in [28]. It encourages each class in L to have high probability on at least one pixel in the image. We extend this loss

to include the second summation over $c \in L'$. This corresponds to the fact that no pixels should have high probability for classes that are not present in the image. We found this simple extension to be very effective in practice.

Point-level supervision. We study the intermediate case where the object classes are known for a small set of supervised pixels \mathcal{I}_s , whereas other pixels are just known to belong to some class in L . In this case, we generalize Eqn. (1) and Eqn. (2) to:

$$\mathcal{L}_{point}(S, G, L, L') = \mathcal{L}_{img}(S, L, L') - \sum_{i \in \mathcal{I}_s} \alpha_i \log(S_{iG_i}) \quad (3)$$

Here, α_i determines the relative importance of each supervised pixel. We experiment with several formulations for α_i . (1), for each class we ask the user to either determine that the class is not present in the image or to point to one object instance. In this case, $|\mathcal{I}_s| = |L|$ and α_i is uniform for every point; (2), we ask multiple annotators to do the same task as (1), and we set α_i to be the confidence of the accuracy of the annotator that provided the point; (3), we ask the annotator(s) to point to every *instance* of the classes in the image, and α_i corresponds to the *order* of the points: the first point is more likely to correspond to the largest object instance and thus deserves a higher weight α_i .

Objectness prior. One issue with training models with very few or no supervised pixels is correctly inferring the spatial extent of the objects. In general, weakly supervised methods are prone to local minima: they focus on only a small part of the target object, or predict all pixels as belonging to the background class [28]. To alleviate this problem, we introduce an additional term in our training objective based on an objectness prior (Fig. 2). Objectness provides a probability for whether each pixel belongs to *any* object class [2] (e.g., bird, car, sheep), as opposed to background (e.g., sky, water, grass). These probabilities have been previously used in the weakly supervised semantic segmentation before as unary potentials in graphical models [37] or during inference following a CNN segmentation [29]. To the best of our knowledge, we are the first to incorporate them directly into CNN training.

We calculate the per-pixel objectness prior by assigning each pixel the average objectness score of all windows containing it. These scores are obtained by using the pre-trained objectness model from the released code of [2]. The objectness model is pre-trained on 50 images randomly sampled from a variety of different datasets (e.g., INRIA Person, Caltech 101) that do not overlap with PASCAL VOC 2007-2012.

Let P_i be the probability that pixel i belongs to an object. Let \mathcal{O} be the classes corresponding to objects, with the other classes corresponding to backgrounds. In PASCAL VOC, \mathcal{O} are the 20 object classes, and there is a single generic



Figure 3: (a) AMT annotation user interface for point-level supervision. (b) Example points collected. Different colors correspond to different classes. (Best viewed in color).

background class. We define a new loss:

$$\mathcal{L}_{obj}(S, P) = -\frac{1}{|\mathcal{I}|} \sum_{i \in \mathcal{I}} P_i \log \left(\sum_{c \in \mathcal{O}} S_{ic} \right) + (1 - P_i) \log \left(1 - \sum_{c \in \mathcal{O}} S_{ic} \right) \quad (4)$$

At pixels with high P_i values, this objective encourages placing probability mass on object classes. Alternatively, when P_i is low, it prefers mass on the background class. Note that \mathcal{L}_{obj} requires no human supervision and thus can be combined with any loss above.

4. Crowdsourcing annotation data

In this section, we describe our method for collecting annotations for the different levels of supervision (image-level labels, points, squiggles, bounding boxes, and full supervision) and comparing their per-image annotation times.

4.1. Collecting point data

Point supervision can be used in training semantic segmentation models as described in Section 3. We collect points for two different tasks: (1) annotators are asked to click on the first instance of the target class they see (*1Point*), and (2) annotators are asked to click on every instance of the target class (*AllPoints*). By running these tasks for all classes and all images, we obtain one annotated point per object class per image (*1Point*), or one annotated point per object instance per image (*AllPoints*).¹

¹Quality control is done by planting 10 evaluation images in a 50-image task and ensuring at least 8 are labeled correctly. We consider a click correct if it falls inside a tight bounding box around the object. For the *AllPoints* task, the number of annotated clicks must be at least the number of known object instances.

We used Amazon Mechanical Turk (AMT) to annotate 20 PASCAL VOC object classes on 12,031 images: all training and validation images of the PASCAL VOC 2012 segmentation task [8] plus the additional images of [14]. Fig. 3 shows some collected data. We will make the collected annotations and annotation system publicly available.

Error rates. Simply determining the presence or absence of an object class in an image was fairly easy, and workers incorrectly labeled an object class as absent only 1.0% of the time. On the *1Point* task, 7.2% of points were on a pixel annotated with a different object class in the ground truth, and an additional 0.8% were on an unclassified “difficult” ground truth pixel. For comparison, [32] reports a higher 25% average error rate when drawing bounding boxes. Our collected data is high-quality, confirming that pointing to objects comes naturally to humans [6, 23]. Annotators had more difficulty with the *AllPoints* class: 7.9% of ground truth instances were left unannotated, 14.8% of the clicks were on the wrong object class, and 1.6% on “difficult” pixels. This task caused some confusion among workers due to blurry or very small instances; for example, many of these instances are not annotated in the ground truth but were clicked by workers, accounting for the high false positive rate. For simplicity, throughout most of the paper we focus on the *1Point* rather than the *AllPoints* data for point-level annotation.

Annotation time. It takes workers approximately 1 second to determine the presence or absence of an object class. Therefore, annotating 20 object classes in PASCAL VOC with image-level labels takes **20** seconds per image. There are 1.5 classes on average per image in PASCAL VOC 2012. It takes workers a median of 2.4 seconds to click on the first instance of an object. Therefore, the labeling cost of *1Point* is $1 \times 18.5 + 2.4 \times 1.5 = \mathbf{22.1}$ seconds per image. If a class is present, there are on average 0.8 additional instances beyond the first one. It takes workers a median of 0.9 seconds to click on every additional instance of an object class. Therefore, the labeling cost of *AllPoints* is $1 \times 18.5 + 1.5(2.4 + 0.9 \times 0.8) = \mathbf{23.2}$ seconds per image. This is only $1.10 - 1.16\times$ more expensive than obtaining image-level labels.

4.2. Stronger modes of supervision

We also wish to compare against three stronger modes of supervision. Below, we compare per-image annotation times for various types of annotations to confirm that point-level supervision is very efficient.

Squiggle-level supervision. [41] has experimented with training with free-form squiggles, where a subset of pixels are labeled. However, [41] simulates squiggles by randomly labeling superpixels from the ground truth, rather than collecting them from humans. In order to properly



Figure 4: Example squiggles collected.

compare this supervision setting to human points, we need to collect both actual human squiggles and annotation times. We extend the user interface shown in Fig. 3 by asking annotators to draw one squiggle on the extent of the target class. Fig. 4 shows some collected data.

Error rates. Workers incorrectly labeled an object class as absent only 0.11% of the time. 6.3% of the clicks were on the wrong object class, and an additional 1.4% were on “difficult” pixels.

Annotation times. As before, it takes 18.5 seconds to annotate the classes not present in the image. For every class that is present, it takes 10.9 seconds to draw a free-form squiggle on the target class. Therefore, the labeling cost of the squiggles task is $18.5 + 1.5 \times 10.9 = 34.9$ seconds per image. This is $1.58\times$ more expensive than obtaining 1Point point-level supervision and $1.75\times$ more expensive than image-level labels.

Box-level supervision. A common intermediate between image-level labels and pixel-wise segmentations is to obtain bounding box annotations around each object instance. We use the bounding boxes provided with the PASCAL VOC dataset, and estimate the annotation times from literature.

Timing greatly depends on the setup. [18] reports 7 seconds to draw a bounding box. However, they do not examine their quality, and carry out their study on rather easy datasets with mainly large centered objects (MSRC, IIS, iCoSeg). [32] reports 10.2 seconds with high AMT error rates. [36] reports 25.5 seconds for drawing and 42.4 seconds with quality verification. The protocol of [36] has been used for producing the official annotations of the ILSVRC [31], which is currently the most popular dataset for object class detection and is of comparable difficulty to PASCAL VOC. Its bounding boxes are high quality and precisely match the object extent. Hence, in this paper we assume it takes 26 seconds to draw a precise bounding box without quality verification. On average, there are a total of 2.8 instances per image over all classes. Therefore, annotating them takes $18.5 + 2.8 \times 26 = 91.3$ seconds. This is $4.1\times$ more expensive than point-level supervision.

Full supervision. For segmentation annotation, the authors of the COCO dataset report 22 worker hours per 1000 segmentations, so 79 seconds per segmentation [21]. Thus to segment all instances it takes $18.5 + 2.8 \times 79 = 239.7$ seconds, more than $10\times$ the cost of point supervision.

In Section 5 we compare the accuracy of the models trained with different levels of supervision.

5. Experiments

We empirically demonstrate the effectiveness of our point-level supervision and objectness prior.

5.1. Setup

CNN architecture. We use the state-of-the-art fully convolutional network model as in [22]. Briefly, the architecture is based on the VGG 16-layer net [34], with all fully connected layers converted to convolutional layers. The last classifier layer is discarded and replaced with a 1×1 convolution layer with channel dimension $N = 21$ equal to the number of object classes. The final modification is the addition of a deconvolution layer to bilinearly upsample the output to pixel-level dense predictions.²

CNN training. We train following a procedure similar to [22]. We use stochastic gradient descent with a fixed learning rate of 10^{-5} , doubling the learning rate for biases, and with a minibatch of 20 images, momentum of 0.9 and weight decay 0.0005. The network is initialized with weights pre-trained for a 1000-way classification task of the ILSVRC 2012 dataset [34, 31, 22].³ In the fully supervised case, we zero-initialize the classifier weights [22], and for all the weakly supervised cases we follow [28] to initialize them with weights learned by the original VGG network for classes common to both PASCAL and ILSVRC. We back-propagate through all layers to fine-tune the network, and train for 50,000 iterations. We build directly upon the publicly available implementation of [22, 19].

Dataset. We train and evaluate on the PASCAL VOC 2012 segmentation dataset [8] augmented with extra annotations from [14]. There are 10,582 training images, 1,449 validation images and 1,456 test images. We report the mean intersection over union (mIOU), averaged over 21 classes. Table 5a gives the performances of our models on the validation set of PASCAL VOC 2012.

5.2. Point-level supervision

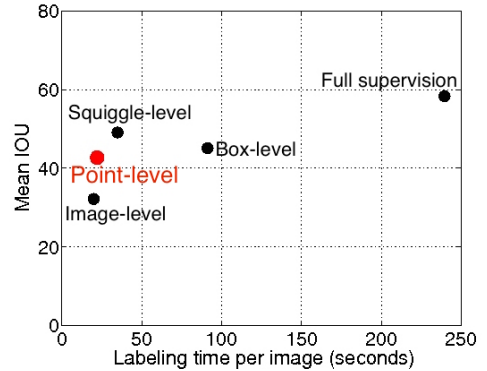
Baseline. We begin by establishing a baseline segmentation model trained from image-level labels with no additional information. We base our model on [28], which trains a similar fully convolutional network and obtains 25.1%

²[22] introduces additional refinement by decreasing the stride of the output layers from 32 pixels to 8 pixels, which improves their results from 59.7% to 62.7% mIOU on the PASCAL VOC 2011 validation set. We use the original model with stride of 32 for simplicity.

³This is standard in the literature [5, 22, 28, 26, 29, 11]. We do not consider the cost of collecting those annotations; including them would not change our overall conclusions.

Supervision	Annotation time (s)	Model	mIOU (%)
Image-level labels	20.0	<i>Img</i>	29.8
Image-level labels	20.0	<i>Img + Obj</i>	32.2
1 <i>Point</i>	22.1	<i>Img</i>	35.1
1 <i>Point</i>	22.1	<i>Img + Obj</i>	42.7
<i>AllPoints</i>	23.2	<i>Img + Obj</i>	42.7
<i>AllPoints</i> (weighted)	23.2	<i>Img + Obj</i>	43.4
1 <i>Point</i> (3 annotators)	29.3	<i>Img + Obj</i>	43.8
1 <i>Point</i> (random)	239.7	<i>Img + Obj</i>	46.1
1 squiggle per class	34.9	<i>Img + Obj</i>	49.1
1 bounding box per instance	91.3	<i>Img</i>	45.1
Full pixel-level supervision	239.7	<i>Img</i>	58.3

(a) Both point-level supervision and objectness prior significantly improve accuracy. The first section corresponds to our baseline model trained on image-level labels, and models trained with point supervision (see Section 5.2). The middle section shows the results of variations of point supervision (see Section 5.3). The last section corresponds to models trained with stronger supervision (see Section 5.4).



(b) Models trained with varying levels of supervision. Point-level supervision trades off well between annotation time and accuracy.

Figure 5: Results on the PASCAL VOC 2012 validation set.

mIOU on the PASCAL VOC 2011 validation set. We notice that the *absence* of a class label in an image is also an important supervisor signal, along with the presence of a class label, as in [27]. We incorporate this insight into our loss function \mathcal{L}_{img} in Eqn. 2, and see a substantial 5.4% improvement in mIOU from the baseline, when evaluated on the PASCAL VOC 2011 validation set.

Effect of point-level supervision. We now run a key experiment to investigate how having just one annotated point per class per image improves semantic segmentation accuracy. We use loss \mathcal{L}_{point} of Eqn. (3). On average there are only 1.5 pixels supervised per image (as many as classes per image). All other pixels are unsupervised. We set $\alpha = 1/n$, where n is the number of supervised pixels on a particular training image. On the PASCAL VOC 2012 validation set, the accuracy of a model trained using \mathcal{L}_{img} is 29.8% mIOU. Adding our point supervision improves accuracy by 5.3% to 35.1% mIOU (row 3 in Table 5a).

Effect of objectness prior. One issue with training models with very few or no supervised pixels is the difficulty of inferring the full extent of the object. With image-level labels, the model tends to learn that objects occupy a much greater area than they actually do (second column of Fig. 6). We introduce the objectness prior in the loss using Eqn. (4) to aid the model in correctly predicting the extent of objects (third column on Fig. 6). This improves segmentation accuracy: when supervised only with image-level labels, the *Img* model obtained 29.8% mIOU, and the *Img + Obj* model improves to 32.2% mIOU.

Synergy between point-level supervision and objectness.

The effect of the objectness prior is even more apparent when used together with point-level supervision. When supervised with 1*Point*, the *Img* model achieves 35.1% mIOU, and the *Img + Obj* model improves to 42.7% mIOU (rows 3 and 4 in Table 5a). Conversely, when starting from the *Img + Obj* image-level model, the effect of a single point of supervision is stronger. Adding just one point per class improves accuracy by 10.5% from 32.2% to 42.7%.

We conclude that (1) The objectness prior is very effective for training these models with no or very few supervised pixels – and this comes with no additional human supervision cost. For the rest of the experiments where not all pixels are labeled (i.e., all but box-level supervision or full supervision), we always use *Img + Obj* together. (2) our two contributions operate in synergetic ways. The combined effects of both point-level supervision and objectness prior is a +13% improvement (from 29.8% to 42.7% mIOU).

5.3. Point-level supervision variations

Having established that a model with 1*Point* supervision achieves 42.7% mIOU, we analyze variations of point-level supervision and compare the trade-offs of accuracy with annotation time (also documented in Table 5a).

Multiple instances. Using points on all instances (*AllPoints*) instead of just one point per class (1*Point*) remains at 42.7% mIOU: the benefit from extra supervision is offset by the confusion introduced by some difficult instances that are annotated. We introduce a weighting factor $\alpha_i = 1/2^r$ in Eqn. (3) where r is the ranked order of the

point (so the first instance of a class gets weight 1, the second instance gets weight 1/2, etc.). This improves results by a modest 0.7% to 43.4% mIOU.

Multiple annotators. We also collected *1Point* data from 3 different annotators and used all points during training. This achieved a modest improvement of 1.1% from 42.7% to 43.8%, which does not seem worth the additional annotation cost (29.3 versus 22.1 seconds per image).

Patches. As mentioned above, the segmentation model is good at extrapolating the full extent of the object, so increasing the area of supervised pixels by a radius of 2, 5, and 25 pixels around a point also has little effect, with 43.0 – 43.1% mIOU (not shown in Table 5a).

Squiggles. We next analyze supervision with free-form squiggles, which are a natural extension of points. [41] also trains weakly-supervised models with squiggles, but they randomly generate these squiggles from the ground truth, whereas we collect them from humans. We collect an average of 502.7 supervised pixels per image with squiggles, vs. 1.5 with *1Point*. Like points, squiggles provide a good trade-off between accuracy and annotation cost. The squiggle-supervised model achieves 19.3% higher mIOU than image-level labels, and 6.4% higher mIOU than *1Point*, at only 1.58× and 1.75× the cost, respectively.

Random points. An interesting experiment is supervising with one point per class but randomly sampled on the target object class using per-pixel supervised ground truth annotations (instead of asking humans to click on the object). This improved results over the human points by 3.4%, from 42.7% to 46.1%. This is due to the fact that humans are predictable and consistent in pointing [10, 6], which reduces the variety in point-level supervision across instances.

5.4. Comparison to stronger supervision

We compare our point-supervised model with models trained with stronger supervision in terms of labeling cost and accuracy. We use the annotation time computed in Section 4: on one image, it takes 20 seconds for image-level, 22.1 seconds for point-level (*1Point*), 34.9 seconds for squiggle-level, 91.3 seconds for bounding boxes, and 239.7 seconds for full per-pixel annotation.⁴ Fig. 5b summarizes the performances of our model trained under different levels of supervision.

⁴ The 50 images used to train the objectness prior are also annotated with 291 total bounding boxes. We do not incorporate this annotation cost for two reasons. First, the added cost of annotating these 50 images with bounding boxes is negligible to the cost of annotating the 12,031 images of PASCAL VOC 2012 with point data (0.808 hours vs. 77.5 hours). Second, we do not include the annotation cost of any generic knowledge learned beforehand, used in publicly available models. For example, we also do not include the annotation cost of CNN models pre-trained on ILSVRC 2012 data, which took hundreds of hours to annotate.

Bounding boxes. To train the bounding box-supervised model we use the bounding box annotations available on PASCAL VOC. We convert them to per-pixel annotations by assuming that each pixel belongs to the object class of the smallest box covering it [26]. The box-supervised model obtains 2.4% higher mIOU than the model supervised with *1Point*, but 4% lower mIOU than the model supervised with squiggles. We use a straightforward approach to bounding box supervision, where pixels inside the bounding box are supervised as belonging to the object class (following a baseline in [26]). More sophisticated techniques, such as only assigning superpixels that are a certain percentage inside the box as the object class [41] or using a CRF to obtain a better segmentation within the box [26], can be applied. These and similar techniques can also be applied to enhance accuracy with point-level supervision; we choose the simplest strategy here to provide an “apples-to-apples” comparison.

Full supervision. The fully supervised model trumps all others in accuracy, with 58.3% mIOU, but at a 10.2× and 6.9× increase in cost compared to our point-level and squiggle-level supervision, respectively.

Fig. 6 compares our model (*Img + Obj* supervised with *1Point*) to our baseline (*Img* supervised with image-level labels) and the fully supervised model. Both models perform well for images of single or discrete objects, with a well-defined foreground/background, as in row 1, right side. Our model sometimes has difficulties predicting the extent of an object, as in row 2, right side, and may overextend its segmentation especially when there are objects of similar colors nearby. In row 3, right side, our model outperforms the fully supervised model because it is encouraged to not predict classes that are not present in the image. Finally, both models achieve low mIOU when the image is very cluttered, and/or contains extra objects that are not among the 20 PASCAL classes but are also not background (row 4, right side).

5.5. Comparison to other techniques

We compare both the annotation time and accuracy of our point-supervised *1Point* model with published techniques. Here we train on all 12,031 train+validation images and evaluate on the PASCAL VOC 2012 test set (as opposed to the validation set above).

Fig. 7 shows the results. Pathak ICLR *et al.* [28] achieves 25.7% mIOU, Pathak ICCV *et al.* [27] achieves 35.6% mIOU, and Papandreou *et al.* [26] achieves 39.6% mIOU with only image-level labels requiring approximately 67 hours of annotation on the 12,301 images (Section 4). Pinheiro *et al.* [29] achieves 40.6% mIOU but with 400 hours of annotations.⁵ We improve in accuracy upon all of these

⁵[29] trains with only image-level annotations but adds 700,000 ad-

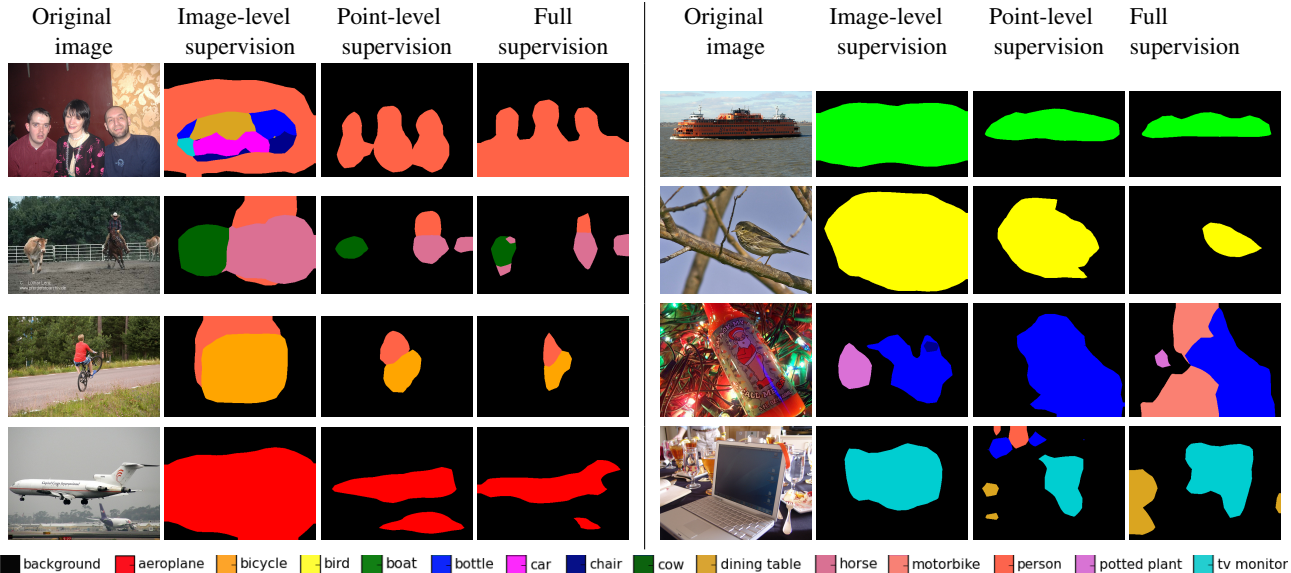


Figure 6: Qualitative results on the PASCAL VOC 2012 validation set. The combination of point-level supervision and the objectness prior yields substantial improvements in accuracy over image-level labels (*Img*), at small additional annotation cost. Note the ability to separate closely interacting objects of the same class (row 1, left) and different classes (row 3, left), and to infer the correct extent of the object(s). Row 4, right shows a failure case, where the point-supervised model incorrectly labels a laptop as a “tv monitor.” Best viewed in color. See the supplementary material for more examples.

methods and achieve 43.6% with point-level supervision requiring about 79 annotation hours (*Img + Obj + 1Point*). Note that our baseline model is a significantly simplified version of [28, 26]. Incorporating additional features of their methods is likely to further increase our accuracy at no additional annotation cost.

Long *et al.* [22] reports 62.2% mIOU, Hong *et al.* [17] reports 66.6% mIOU, and Chen *et al.* [5] reports 71.6% mIOU, but in the fully supervised setting that requires about 800 hours of annotation, an order of magnitude more expensive than point supervision.

6. Conclusion

In this paper, we propose a new supervision approach for semantic image segmentation based on humans pointing to objects. With just a small handful of manually annotated pixels, we considerably improve semantic segmentation accuracy. In addition, we introduce an objectness prior directly in the loss function of our CNN to help infer the extent of the object. We demonstrated the effectiveness of our approach by evaluating on the PASCAL VOC 2012 dataset. The combination of point supervision and the objectness

ditional positive ImageNet images and 60,000 background images. We choose not to count the 700,000 freely available images but the additional 60,000 background images they annotated would take an additional $60,000 \times 20 \text{ classes} \times 1 \text{ second} = 333$ hours. The total annotation time is thus $333 + 67 = 400$ hours.

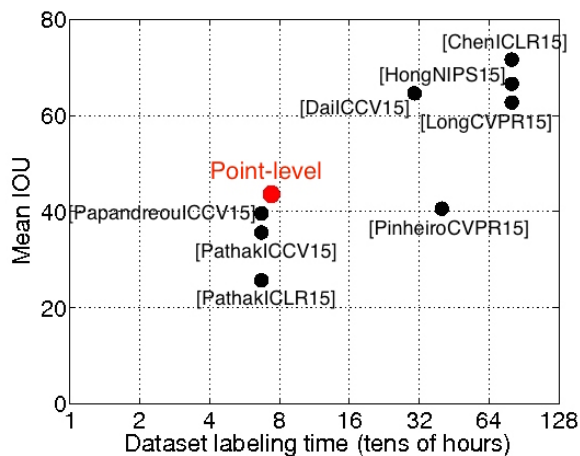


Figure 7: Results on the PASCAL VOC 2012 test set. Our model outperforms [29] on both accuracy and labeling cost, and [26, 28, 27] on accuracy at a 10% increase in labeling cost.

prior outperforms models trained on image-level labels by a significant 12.9% mean intersection over union, with negligible additional labeling cost.

References

- [1] E. Ahmed, S. Cohen, and B. Price. Semantic object selection. In *CVPR*, 2014. 1, 2
- [2] B. Alexe, T. Deselares, and V. Ferrari. Measuring the objectness of image windows. In *PAMI*, 2012. 2, 3
- [3] S. Bell, P. Upchurch, N. Snavely, and K. Bala. Material recognition in the wild with the materials in context database. *Computer Vision and Pattern Recognition (CVPR)*, 2015. 1, 2
- [4] Y. Chai, V. Lempitsky, and A. Zisserman. BiCoS: A bi-level co-segmentation method for image classification. In *CVPR*, 2011. 2
- [5] L.-C. Chen, G. Papandreou, I. Kokkinos, K. Murphy, and A. L. Yuille. Semantic image segmentation with deep convolutional nets and fully connected CRFs. In *ICLR*, 2015. 2, 3, 5, 8
- [6] H. H. Clark. Coordinating with each other in a material world. *Discourse Studies*, 7(4-5):507–525, 2005. 1, 4, 7
- [7] J. Dai, K. He, and J. Sun. Boxesup: Exploiting bounding boxes to supervise convolutional networks for semantic segmentation. *arXiv preprint arXiv:1503.01640*, 2015. 2
- [8] M. Everingham, L. Van Gool, C. K. I. Williams, J. Winn, and A. Zisserman. The Pascal Visual Object Classes (VOC) challenge. *IJCV*, 88(2):303–338, June 2010. 2, 3, 4, 5
- [9] C. Farabet, C. Couprie, L. Najman, and Y. LeCun. Learning hierarchical features for scene labeling. *TPAMI*, August 2013. 1, 2
- [10] C. Firestone and B. J. Scholl. Please Tap the Shape, Anywhere You Like: Shape skeletons in human vision revealed by an exceedingly simple measure. *Psychological Science*, 25(2):377386, 2014. 1, 7
- [11] R. Girshick, J. Donahue, T. Darrell, and J. Malik. Rich feature hierarchies for accurate object detection and semantic segmentation. In *CVPR*, 2014. 1, 5
- [12] S. Gould. Multiclass pixel labeling with non-local matching constraints. In *CVPR*, 2012. 1
- [13] M. Guillaumin, D. Kuettel, and V. Ferrari. ImageNet Auto-annotation with Segmentation Propagation. *IJCV*, 2015. 1, 2
- [14] B. Hariharan, P. Arbelaez, L. Bourdev, S. Maji, and J. Malik. Semantic contours from inverse detectors. In *ICCV*, 2011. 4, 5
- [15] B. Hariharan, P. Arbeláez, R. Girshick, and J. Malik. Simultaneous detection and segmentation. In *ECCV*, 2014. 2
- [16] M. Hild, M. Hashimoto, and K. Yoshida. Object recognition via recognition of finger pointing actions. In *Image Analysis and Processing*, pages 88–93, 2003. 1, 2
- [17] S. Hong, H. Noh, and B. Han. Decoupled deep neural network for semi-supervised semantic segmentation. In *Advances in Neural Information Processing Systems 28*, 2015. 2, 8
- [18] S. D. Jain and K. Grauman. Predicting sufficient annotation strength for interactive foreground segmentation. In *ICCV*, December 2013. 1, 5
- [19] Y. Jia, E. Shelhamer, J. Donahue, S. Karayev, J. Long, R. Girshick, S. Guadarrama, and T. Darrell. Caffe: Convolutional architecture for fast feature embedding. In *Proceedings of the ACM International Conference on Multimedia*, pages 675–678. ACM, 2014. 5
- [20] A. Joulin, F. Bach, and J. Ponce. Discriminative clustering for image co-segmentation. In *CVPR*, 2010. 2
- [21] T.-Y. Lin, M. Maire, S. Belongie, J. Hays, P. Perona, D. Ramanan, P. Dollr, and C. L. Zitnick. Microsoft COCO: Common Objects in Context. In *ECCV*, 2014. 1, 5
- [22] J. Long, E. Shelhamer, and T. Darrell. Fully convolutional networks for semantic segmentation. In *CVPR*, 2015. 1, 2, 3, 5, 8
- [23] D. Merrill and P. Maes. Augmenting looking, pointing and reaching gestures to enhance the searching and browsing of physical objects. In *Pervasive Computing, Lecture Notes in Computer Science*. 2007. 1, 2, 4
- [24] H. Noh, S. Hong, and B. Han. Learning deconvolution network for semantic segmentation. In *Computer Vision (ICCV), 2015 IEEE International Conference on*, 2015. 2
- [25] D. P. Papadopoulos, A. D. F. Clarke, F. Keller, and V. Ferrari. Training object class detectors from eye tracking data. In *ECCV*, 2014. 1, 2
- [26] G. Papandreou, L.-C. Chen, K. Murphy, and A. L. Yuille. Weakly- and semi-supervised learning of a deep convolutional network for semantic image segmentation. 1, 2, 5, 7, 8
- [27] D. Pathak, P. Krähenbühl, and T. Darrell. Constrained convolutional neural networks for weakly supervised segmentation. 2015. 1, 2, 6, 7, 8
- [28] D. Pathak, E. Shelhamer, J. Long, and T. Darrell. Fully convolutional multi-class multiple instance learning. In *ICLR*, 2015. 1, 2, 3, 5, 7, 8
- [29] P. O. Pinheiro and R. Collobert. From image-level to pixel-level labeling with convolutional networks. In *CVPR*, 2015. 1, 2, 3, 5, 7, 8
- [30] C. Rother, V. Kolmogorov, and A. Blake. GrabCut: Interactive foreground extraction using iterated graph cuts. In *ACM SIGGRAPH*, 2004. 1, 2
- [31] O. Russakovsky, J. Deng, et al. ImageNet Large Scale Visual Recognition Challenge. *IJCV*, 2015. 1, 5
- [32] O. Russakovsky, L.-J. Li, and L. Fei-Fei. Best of both worlds: human-machine collaboration for object annotation. In *CVPR*, 2015. 4, 5
- [33] A. Sauppe and B. Mutlu. Robot deictics: how gesture and context shape referential communication. In *HRI'14*, pages 342–349, 2014. 2
- [34] K. Simonyan and A. Zisserman. Very deep convolutional networks for large-scale image recognition. In *ICLR*, 2015. 1, 5
- [35] H. O. Song, R. Girshick, S. Jegelka, J. Mairal, Z. Harchaoui, and T. Darrell. On learning to localize objects with minimal supervision. In *ICML*, 2014. 1
- [36] H. Su, J. Deng, and L. Fei-Fei. Crowdsourcing annotations for visual object detection. In *AAAI Human Computation Workshop*, 2012. 5
- [37] A. Vezhnevets, V. Ferrari, and J. Buhmann. Weakly supervised semantic segmentation with a multi-image model. In *ICCV*, 2011. 1, 2, 3

- [38] A. Vezhnevets, V. Ferrari, and J. Buhmann. Weakly supervised structured output learning for semantic segmentation. In *CVPR*, 2012. [1](#)
- [39] T. Wang, B. Han, and J. Collomosse. Touchcut: Fast image and video segmentation using single-touch interaction. *CVIU*, 120, 2014. [1](#), [2](#)
- [40] J. Xu, A. G. Schwing, and R. Urtasun. Tell Me What You See and I will Show You Where It Is. In *CVPR*, 2014. [1](#)
- [41] J. Xu, A. G. Schwing, and R. Urtasun. Learning to segment under various forms of weak supervision. In *CVPR*, 2015. [1](#), [2](#), [4](#), [7](#)